

AIR FORCE WRIGHT AERONAUTICAL LABS WRIGHT-PATTERSON AFB OH F/G 20/7  
80-MICRON PARTICLE ACCELERATION IN AN EXPANDING GAS. (U)

NOV 81 S H HASINGER  
AFWAL-TR-81-3105

NL

17  
2025

END  
DATE  
FILMED  
3 82  
DTIC

AFWAL-TR-81-3105

LEVEL 1



AD A110865

# 80-MICRON PARTICLE ACCELERATION IN AN EXPANDING GAS

Siegfried H. Hasinger

Thermomechanics Branch  
Aeromechanics Division

November 1981

Interim Report for Period February 1980 - October 1980

Approved for public release; distribution unlimited.

DTIC FILE COPY

FLIGHT DYNAMICS LABORATORY  
AIR FORCE WRIGHT AERONAUTICAL LABORATORIES  
AIR FORCE SYSTEMS COMMAND  
WRIGHT-PATTERSON AFB, OH 45433

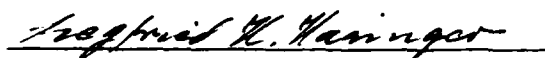
DTIC  
LECTE  
FEB 12 1982  
A

NOTICE

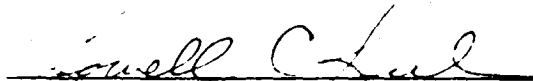
When Government drawings, specifications, or other data are used for any purpose other than in connection with a definitely related Government procurement operation, the United States Government thereby incurs no responsibility nor any obligation whatsoever; and the fact that the government may have formulated, furnished, or in any way supplied the said drawings, specifications, or other data, is not to be regarded by implication or otherwise as in any manner licensing the holder or any other person or corporation, or conveying any rights or permission to manufacture use, or sell any patented invention that may in any way be related thereto.

This report has been reviewed by the Office of Public Affairs (ASD/PA) and is releasable to the National Technical Information Service (NTIS). At NTIS, it will be available to the general public, including foreign nations.

This technical report has been reviewed and is approved for publication.



SIEGFRIED H. HASINGER  
Aerosp Engr, Aerodynamics & Airframe Br  
Aeromechanics Division



LOWELL C. KEEL, MAJ, USAF  
Chief, Aerodynamics & Airframe Br  
Aeromechanics Division

FOR THE COMMANDER



JOHN R. CHEVALIER  
Colonel, USAF  
Chief, Aeromechanics Division

"If your address has changed, if you wish to be removed from our mailing list, or if the addressee is no longer employed by your organization please notify AFWAL/FIMM, W-PAFB, OH 45433 to help us maintain a current mailing list".

Copies of this report should not be returned unless return is required by security considerations, contractual obligations, or notice on a specific document.

Unclassified

SECURITY CLASSIFICATION OF THIS PAGE (When Data Entered)

REPORT DOCUMENTATION PAGE		READ INSTRUCTIONS BEFORE COMPLETING FORM
1. REPORT NUMBER AFWAL-TR-81-3105	2. GOVT ACCESSION NO. AD-A110 865	3. RECIPIENT'S CATALOG NUMBER
4. TITLE (and Subtitle) 80-MICRON PARTICLE ACCELERATION IN AN EXPANDING GAS		5. TYPE OF REPORT & PERIOD COVERED Interim Report February 1980 - October 1980
		6. PERFORMING ORG. REPORT NUMBER
7. AUTHOR(s) Siegfried H. Hasinger		8. CONTRACT OR GRANT NUMBER(s)
9. PERFORMING ORGANIZATION NAME AND ADDRESS Flight Dynamics Laboratory (AFWAL/FIME) Air Force Wright Aeronautical Laboratories, AFSC Wright-Patterson Air Force Base, Ohio 45433		10. PROGRAM ELEMENT, PROJECT, TASK AREA & WORK UNIT NUMBERS Project 2404 Task 240404 Work Unit 240404-09
11. CONTROLLING OFFICE NAME AND ADDRESS Flight Dynamics Laboratory (AFWAL/FIME) Air Force Wright Aeronautical Laboratories Wright-Patterson Air Force Base, Ohio 45433		12. REPORT DATE November 1981
		13. NUMBER OF PAGES 39
14. MONITORING AGENCY NAME & ADDRESS (if different from Controlling Office)		15. SECURITY CLASS. (of this report) Unclassified
		15a. DECLASSIFICATION DOWNGRADING SCHEDULE N/A
16. DISTRIBUTION STATEMENT (of this Report)  Approved for public release; distribution unlimited.		
17. DISTRIBUTION STATEMENT (of the abstract entered in Block 20, if different from Report)		
18. SUPPLEMENTARY NOTES		
19. KEY WORDS (Continue on reverse side if necessary and identify by block number) Particle Acceleration Gas Expansion with Wall Friction Gas Expansion with Heat Loss Flow Profile Shape		
20. ABSTRACT (Continue on reverse side if necessary and identify by block number) For the purpose of re-entry erosion testing, small particles (80-micron size) can be accelerated to high speeds in expanding helium. To provide sufficient residence time of the particles in the flow for an effective acceleration process, the necessary expansion nozzles become very long relative to their throat diameter, with the consequence of incurring considerable wall friction losses. A method is presented for calculating flow expansion with the inclusion of wall friction forces. This method uses a stepwise procedure which allows a ready account of the particle acceleration process. Since extreme high		

DD FORM 1 JAN 73 1473 EDITION OF 1 NOV 65 IS OBSOLETE

Unclassified

SECURITY CLASSIFICATION OF THIS PAGE (When Data Entered)

Unclassified

SECURITY CLASSIFICATION OF THIS PAGE(When Data Entered)

Block 20 ABSTRACT

gas temperatures (obtained by electric arc heating) must be applied to accomplish required gas speeds the expansion nozzles must be cooled. Nozzle heat losses are also included in the calculations. Optimum nozzle geometries are evaluated.

Unclassified

SECURITY CLASSIFICATION OF THIS PAGE(When Data Entered)

FOREWORD

This report covers investigations carried out in support of the ERNT facility operations during the period of 1 February to 31 October 1980 under Work Unit 24040409 of Project 2404 in the Thermomechanics Branch, Aeromechanics Division, Flight Dynamics Laboratory.

The author would like to thank Mr. Kenneth Cramer for his valuable advice in this matter and Mr. Werner Kachel for his generous support of the investigations as Technical Manager of the Facility Technology Group.



10-10-81	<input checked="checked" type="checkbox"/>
10-10-81	<input type="checkbox"/>
10-10-81	<input type="checkbox"/>
10-10-81	<input type="checkbox"/>
Classification	
Distribution/	
Availability Codes	
Availability and/or	
Special	
A	

## TABLE OF CONTENTS

SECTION		PAGE
I	INTRODUCTION	1
II	EXPANSION NOZZLE FLOW CALCULATIONS	3
	1. Flow Expansion in Terms of Fluid Forces	3
	2. Inclusion of Wall Friction Forces	5
III	THE PARTICLE ACCELERATION PROCESS	9
	1. Segmental Calculation Procedure	9
	2. Segment Selection	11
IV	NOZZLE HEAT LOSSES	13
V	CALCULATION RESULTS	16
VI	FLOW PROFILE CONSIDERATIONS	21
	1. General Discussions	21
	2. Peak Mach Number	21
VII	CONCLUSIONS	25

## LIST OF ILLUSTRATIONS

FIGURE		PAGE
1	Fluid Pressure Forces in a Flow Duct Element (supersonic expansion)	29
2	Comparison of Segmental Flow Calculations with Isentropic Flow Conditions for Zero Wall Friction	30
3	Particle Acceleration Models	31
	a. Constant Gas Velocity	31
	b. Increasing Gas Velocity	31
4	Particle Accelerations Calculated with the Simplified Method (illustrated in Figure 3a and used for the example calculations in Section V) Compared with Results Obtained with the More Accurate Method Illustrated in Figure 3b	32
5	Segmental Axisymmetric Nozzle Geometry	32
6	Flow Conditions, Heat Loss, and Particle Acceleration for the Subsonic Portion of the Expansion Nozzles Considered in Figures 7a to c for Their Supersonic Nozzle Portions	33
7	Flow Conditions, Heat Loss, and Particle Acceleration for Various Supersonic Nozzle Configurations (for subsonic nozzle portion see Figure 6)	34
	a. Nozzle Wall Angle $0.34^\circ$	34
	b. Nozzle Wall Angle $0.34^\circ$ and $0.5^\circ$	35
	c. Nozzle Wall Angle $0.34^\circ$ and $0.7^\circ$	36
8	Case of Figure 7a with Particles Injected Downstream of the Nozzle Throat.	37
9	Schematic Flow Profile	38
10	Plot for Determining Peak Mach Numbers from Effective Mach Numbers for Given Flow Profile Shapes	39

## LIST OF SYMBOLS

## GENERAL:

$A$	cross-sectional area
$D$	nozzle diameter
$L$	nozzle length
$\Delta L$	nozzle segment length
$M$	flow Mach number
$p$	static pressure
$R$	gas constant
$T$	static temperature
$V$	gas velocity
$\beta$	wall angle of axisymmetric nozzle
$\gamma$	ratio of spec. heats
$\rho$	density

## INDICES:

0	refers to stagnation condition
1	refers to nozzle segment inlet
2	refers to nozzle segment exit
*	refers to nozzle throat

## SPECIAL FOR SECTION II:

$\alpha$	see Equation 18
$c_f$	pipe friction coefficient
$c$	see Equation 17
$B$	see Equation 10
$E$	see Equation 15
$F_f$	wall friction force

LIST OF SYMBOLS (Continued)

SPECIAL FOR SECTION II:

$I$	flow momentum
$i$	shape factor for pressure distribution along nozzle
$t$	segment exit to inlet area ratio
$\tau$	fluid force parameter (Equation 4)

SPECIAL FOR SECTION III:

$b$	see Equation 27
$c_D$	particle drag coefficient
$d$	particle diameter
$k$	see Equation 26
$s$	length variable within segment
$v_1'$	gas velocity at segment inlet
$v_1''$	gas velocity at segment exit
$v_2'$	particle velocity at segment inlet
$v_2''$	particle velocity at segment exit
$\rho_g$	gas density
$\rho_p$	particle density

SPECIAL FOR SECTION IV:

$(c_f)_{\text{wall}}$	wall friction coefficient
$(c_f)_{\text{pipe}}$	pipe friction coefficient
$d$	nozzle wall thickness
$h$	heat transfer coefficient
$k$	thermal conductivity of gas

## LIST OF SYMBOLS (Continued)

## SPECIAL FOR SECTION IV:

$k_{Cu}$	thermal conductivity of copper
$m$	momentary mass of gas in nozzle segment
$Nu$	Nusselt number
$Q_{loss}$	accumulated heat loss from nozzle
$\Delta Q_{loss}$	heat loss from nozzle segment
$Q_{flux}$	heat flow through unit area of nozzle wall
$Re$	flow Reynolds number
$S$	wall surface area
$(T)_0$	local total gas temperature
$T_{wall}$	nozzle wall temperature
$T_{water}$	cooling water temperature
$\Delta T$	temperature difference between nozzle wall and average boundary layer temperature
$\Delta t$	residence time of gas in nozzle segment
$v$	gas velocity
$\rho_g$	gas density
$\delta_{rec}$	wall temperature recovery factor

## SPECIAL FOR SECTION V:

$Re_f$	flow Reynolds number = $\frac{v_g D \rho_g}{\mu_g}$
$Re_p$	particle Reynolds number = $\frac{(v_g - v_p) d \rho_g}{\mu_g}$
$v_g$	gas velocity
$v_p$	particle velocity

LIST OF SYMBOLS (Concluded)

SPECIAL FOR SECTION VI:

$a$	auxiliary parameter (Equation 48)
$d$	diameter (Figure 9)
$h$	height (Figure 9)
$M_p$	local Mach number of the flow profile (Figure 9)
$M_{eff}$	effective Mach number given by the exit flow momentum
$M_{max}$	peak Mach number of flow profile
$V$	volume

## SECTION I

### INTRODUCTION

Certain re-entry erosion experiments require the acceleration of 80-micron size particles to velocities of several thousand meters per second. A suitable way to produce such high speed particles is to accelerate them in an expanding gas flow. The fluid dynamic design of the necessary expansion nozzles encounters some difficulties. Eighty-micron particles are large as far as particle acceleration in a gas flow is concerned requiring a long residence time and thus, a long path length in the gas for the acceleration process. Practical path lengths are in the order of 1 foot. However, to obtain a sufficiently high gas velocity, helium at high pressure and temperature is used as an operating medium. The scarcity of helium and the great extent of the electric equipment associated with the heating of the gas (1 megawatt arc heater) hold the nozzle mass flow, i.e., the nozzle diameter down (4 mm throat diameter). The resulting expansion nozzles are very slender with the consequence that the expanding gas is exposed to considerable friction on the walls. Determining the wall friction influence becomes a major portion of the design process.

For the present nozzle design a calculation method is used which expresses the expansion process in a given duct in terms of the occurring fluid forces. This method allows a ready inclusion of wall friction forces. To obtain a particularly realistic account of the wall friction influence, this method is applied in steps to consecutive segments of the expansion nozzle with each segment taken small enough that (for the purpose of determining the friction forces) it can be treated as a cylindrical pipe section. The segmental treatment of the expansion process also accommodates the calculation of the particle acceleration. Another advantage of this treatment is that it allows a ready account of the heat losses from the wall. Because of the extremely high expansion temperatures produced by the electric arc (3200°K), the expansion nozzles must be water-cooled with a considerable loss of heat from the nozzles.

In principle the description of a flow process in terms of the occurring fluid forces allows a completely consistent presentation of the expansion process. The resulting expansion Mach number is, together with the expansion pressure, representative for the exit flow momentum and constitutes an average flow Mach number. To obtain peak Mach numbers an assumption about the flow profile shape is required. The present particle acceleration calculations use the average Mach number given by the flow momentum. Therefore, the resulting particle velocities are also average values.

The practical difficulty with applying the present calculation method lies in the choice of the wall friction coefficient. Wall friction is a complex function of flow Reynolds number, flow Mach number, and flow history. The primary purpose of the present calculations was to compare particle velocities obtained with different nozzle geometries. Since deviations from accurate friction values enter the comparison only as secondary effects, constant wall friction coefficients which distinguish only between subsonic and supersonic flow conditions were chosen. On the same grounds the particle drag coefficient was assumed constant, in this case for the entire range of the expansion.

Here the wall friction is expressed in terms of the pipe friction coefficient. Since this coefficient is commonly referred to average flow conditions derived from flow continuity, the Mach number used here satisfies continuity and is particularly suitable for determining wall friction by means of the pipe friction coefficient.

For the purpose of comparing the effect of nozzle geometries on the obtainable particle velocities it was not considered necessary to include mutual interference between particles and the influence of the particles on the gas flow.

## SECTION II

### NOZZLE FLOW CALCULATIONS

#### 1. FLOW EXPANSION IN TERMS OF FLUID FORCES

The balance between flow momentum and fluid pressure forces in a duct with varying cross-sectional area forms the basis for the following derivations. For a duct with inlet cross-sectional area  $A_1$  and exit cross-sectional area  $A_2$  as pictured in Figure 1 for supersonic expansion in a parallel sidewall nozzle, the relation between inlet momentum  $I_1$  and exit momentum  $I_2$  can be written with  $p_1$  and  $p_2$  denoting inlet and exit pressure

$$I_1 = I_2 - A_2 (p_1 - p_2) - (A_1 - A_2) \frac{p_1 - p_2}{2} i \quad (1)$$

This equation is equally applicable to a subsonic expansion nozzle by a consistent use of the signs. Actually, the equation is valid for any type of adiabatic duct flow such as a sudden duct enlargement or a supersonic shock diffuser. The fluid forces acting in the axial direction as a result of the pressure difference in the flow between the duct walls and the exit plane are expressed here with the help of a kind of shape factor designated in Equation 1 with  $i$ . It is introduced into the calculations by the substitution

$$\int_{A_2}^{A_1} (p_1 - p) dA = (A_1 - A_2) \frac{p_1 - p_2}{2} i \quad (2)$$

i. e., the pressure force is calculated in a linearized way by multiplying the wall area projected in the axial direction with the median value of the pressure difference existing between the inlet and exit of the duct element. The factor  $i$  serves as a means to account for the difference between the true integral and the linearized calculation.

For a straight line pressure distribution in a duct configuration as shown in Figure 1, the factor  $i$  is one. In general, pressure distributions in expansion nozzles are different from a straight line and vary in shape with expansion conditions and also with the shape of the duct cross section. The further development of Equation 2 leads to an important involvement of the factor  $i$  in characterizing flows in ducts for the present calculation method. Setting  $A_2/A_1 = t$ , Equation 1 can be written

$$I_1 = I_2 + (p_2 - p_1)A_2\left(\frac{i}{2t} + 1 - \frac{i}{2}\right) \quad (3)$$

The expression in parentheses, abbreviated in the following by writing

$$\tau = \frac{i}{2t} + 1 - \frac{i}{2} \quad (4)$$

becomes the sole criterion for characterizing the type of adiabatic duct flow to which Equation 3 is applied. For instance, for a constant area supersonic diffuser it is  $\tau = 1$  since  $t = 1$ . For a sudden enlargement of a duct from  $A_1$  to  $A_2$ , it is  $\tau = 1/t$  as can be derived from Equation 3. Equation 3 can also be extended to account for a second fluid mixing with the first one as it occurs in an ejector pump. For ejector mixing  $\tau$  can again be treated as a constant known from experiments. Supersonic diffusers and ejectors have been treated in connection with other investigations (Reference 1 and 2). For an adiabatic expansion process (which is of interest here)  $\tau$  must, in general, be determined in each case separately from the expansion conditions (Reference 2). However, as pointed out in the Introduction, for the present case the calculations are applied in a stepwise fashion to small segments of the nozzle and  $\tau$  can also be assigned a unique value. If the considered nozzle segment is short enough, in particular if the pressure drop across the segment is small, the pressure distribution over the length of the segment approaches a straight line, i. e.,  $i$  approaches unity with the influence of the nozzle cross-section shape in  $i$  also disappearing. Then

$$\tau = \frac{t + 1}{2t} \quad (5)$$

At the end of this Section it will be shown that this simplified approach leads to very accurate results for the overall expansion in a nozzle if applied successively to small segments of the expansion nozzle. Equation 3 will be further developed with  $\tau$  considered as a known magnitude according to Equation 5 by the geometry of the contemplated segment of the nozzle.

## 2. INCLUSION OF THE WALL FRICTION FORCES

Considering the generally known relation

$$I = A p \gamma M^2 \quad (6)$$

with  $\gamma$  as the ratio of specific heats and  $M$  as the Mach number of the gas flow Equation 3 becomes with the inclusion of the wall friction forces

$F_f$

$$A_1 p_1 \gamma M_1^2 = A_2 p_2 \gamma M_2^2 + \tau A_2 (p_2 - p_1) + F_f \quad (7)$$

The wall friction forces can be expressed in terms of the common pipe friction coefficient in the following form

$$F_f = A \cdot c_f \cdot \rho \cdot \frac{v^2}{2} \cdot \frac{L}{D} \quad (8)$$

or introducing the flow Mach number

$$F_f = \frac{c_f L}{2 D} p_2 \gamma M_2^2 A_2 \quad (9)$$

For the pipe as a constant geometry duct the inlet is the obvious choice as the reference location for the friction coefficient since the flow conditions are normally given for this location in case of a normal pipe. For a duct with changing cross section as treated here, the choice of reference cross section depends on the significance of the flow conditions for the overall wall friction in the chosen duct segment. The

present calculation method has been originally derived for treating ejector systems. For the ejector, the mixed flow, i.e., the exit flow is more influential for the overall wall friction than the inlet flow where only the slow moving induced flow is in touch with the wall. The exit of the ejector mixing section is therefore the logical choice for the friction coefficient reference location (Reference 1). For an expansion nozzle the choice becomes more arbitrary, particularly, if the calculations are applied to very short segments of the nozzle as proposed here. To allow a consistent use of the originally derived equations the exit of the segment was chosen as the reference location.

Equation 7 can now be transformed into

$$\frac{\gamma \cdot M_1^2}{t} + \tau = \frac{P_2}{P_1} \left[ \gamma M_2^2 \left( \frac{C_f L}{2D} + 1 \right) + \tau \right] \equiv B \quad (10)$$

This equation contains two unknowns: the exit Mach number  $M_2$  and the pressure ratio across the expanding flow. Conservation of mass and energy as expressed by the following relations

$$v_1 \cdot A_1 \cdot \rho_1 = v_2 \cdot A_2 \cdot \rho_2 \quad (11)$$

$$\rho = \frac{P}{RT} \quad (12)$$

$$\frac{T_2}{T_0} = 1 + \frac{\gamma-1}{2} M_2^2 \quad (13)$$

allows one to write an additional condition for determining the two unknowns. Equations 11 through 13 yield the following relation

$$M_2 \left( 1 + \frac{\gamma-1}{2} M_2^2 \right)^{1/2} = \frac{M_1}{t} \frac{P_1}{P_2} \sqrt{\frac{T_0}{T_1}} \quad (14)$$

Solving Equation 10 for  $p_1/p_2$  and introducing it into Equation 14 leads to the basic equation of our flow problem

$$\frac{M_2(1 + \frac{\gamma-1}{2} M_2^2)^{1/2}}{\gamma M_2^2(\frac{c_f L}{2D} + 1) + \tau} = \frac{M_1}{B \cdot t} \sqrt{\frac{T_0}{T_1}} \equiv E \quad (15)$$

This equation can be solved for the exit Mach number

$$M_2^2 = \frac{1 - \left[ \pm \sqrt{1 - \frac{\alpha \tau^2}{c} \left( 2 \frac{c}{\tau} + \frac{1}{\gamma} - 1 \right)} + \alpha \tau \right]}{c \alpha \gamma - \gamma + 1} \quad (16)$$

using the abbreviations

$$c = 1 + \frac{c_f L}{2D} \quad (17)$$

$$\alpha = 2 \gamma E^2 c \quad (18)$$

The magnitude  $E$  in Equation 18 stands for the expression on the right side of Equation 15. The expansion pressure ratio with Equation 10 becomes

$$\frac{p_2}{p_1} = \frac{\frac{\gamma M_1^2}{t} + \tau}{\gamma M_2^2 c + \tau} \quad (19)$$

Equations 16 through 19 are applicable to any adiabatic duct flow including flow mixing, in which case only the right side of Equation 15 assumes a different form. The positive root in Equation 16 yields the subsonic and if applicable, the negative root the supersonic solution of the flow problem. The pipe friction coefficient in Equation 17 is a commonly known function of the flow Reynolds number and the wall surface roughness. As indicated before  $\tau$  is found from Equation 5.

Equation 16 can be applied to any two cross sections of a complete supersonic expansion nozzle consisting of a subsonic and a supersonic portion. The determination of  $\tau$  requires a more complex procedure if the restriction to small segments, i. e., to small flow changes is not maintained. The necessary relations, which are of no interest here, have been derived previously in connection with other investigations (Reference 2).

In Figure 2, Equations 16 and 19 are evaluated for zero wall friction losses using Equation 5 for determining  $\tau$ . Slightly different curves result depending on the choice of the segment length  $\Delta L$ . For comparison, results obtained with exact  $\tau$  values are also entered. As expected on the basis of the definition of  $\tau$ , the exact results are independent of the segment length. They are also in exact agreement with the values obtained from the common isentropic expansion relations. From Figure 2 one sees that for practical purposes the segmental calculation method using a simplified  $\tau$ -value yields very satisfactory results for a proper choice of the segment lengths.

### SECTION III

#### THE PARTICLE ACCELERATION PROCESS

##### 1. SEGMENTAL CALCULATION PROCESS

The acceleration of a particle in a gas flow can be based on the consideration that the work done on the particle by the drag forces over a certain path length must appear again as kinetic energy addition to the particle. Using the notations given in Figure 3a this condition can be expressed by the following relation

$$(v_1' - v_2')^2 c_D \frac{\rho_g}{2} \left(\frac{d}{2}\right)^2 \pi \Delta L = \frac{1}{2} \rho_p \frac{4}{3} \pi \left(\frac{d}{2}\right)^3 [(v_2'')^2 - (v_2')^2] \quad (20)$$

or with some rearrangement

$$\Delta L (v_1' - v_2')^2 = \frac{2}{3} \frac{\rho_p d}{\rho_g c_D} [(v_2'')^2 - (v_2')^2] \quad (21)$$

In this approach any change of the gas velocity within the particle path  $\Delta L$  is neglected. It will be shown later that this simplified approach is still admissible for the case of the expanding flow, i.e., for an increasing gas velocity, if  $\Delta L$  is chosen sufficiently small.

Equation 21 can be developed further by solving it for  $v_2''$  and dividing both sides with  $v_1''$

$$\frac{v_2''}{v_1''} = \frac{v_1'}{v_1''} \sqrt{\Delta L \frac{\rho_g c_D}{\rho_p d} \frac{3}{2} \left(1 - \frac{v_2'}{v_1'}\right)^2 + \left(\frac{v_2'}{v_1'}\right)^2} \quad (22)$$

The velocity ratio obtained with this relation is the exit velocity ratio of the contemplated segment and thus the inlet velocity ratio for the following segment.

To check the accuracy of Equation 22, a more elaborate relation which takes the change of the flow velocity in the segment into account, was also derived. The pertinent acceleration model is shown in Figure 3b. The conditions for this model can be written in the following differential form

$$(v_1 - v_2)^2 c_D \frac{\rho_g}{2} \left(\frac{d}{2}\right)^2 \pi ds = \frac{1}{2} \rho_p \frac{4}{3} \pi \left(\frac{d}{2}\right)^3 \left[ (v_2 + dv_2)^2 - v_2^2 \right] \quad (23)$$

or solved for ds

$$ds = \frac{\rho_p d}{\rho_g c_D} \frac{2}{3} \frac{\left[ (v_2 + dv_2)^2 - v_2^2 \right]}{(v_1 - v_2)^2} \quad (24)$$

By replacing the  $v_1$ -curve in Figure 3b by a straight line within the segment considered,  $v_1$  in Equation 24 can be expressed by

$$v_1 = v_1' + (v_1'' - v_1') \frac{s}{\Delta L} \quad (25)$$

Equation 24 with substituting

$$\frac{\rho_p d}{\rho_g c_D} \frac{2}{3} = k \quad (26)$$

$$\left( \frac{v_1''}{v_1'} - 1 \right) = b \quad (27)$$

becomes

$$ds = k \frac{2 v_2 dv_2 + (dv_2)^2}{\left( v_1' - v_2 + v_1' \frac{b s}{\Delta L} \right)^2} \quad (28)$$

considering that  $(dv_2)^2$  in this equation is of second order influence,

it can be neglected and the equation becomes with dividing numerator and denominator by  $(v_1')^2$

$$ds = \frac{2 k \frac{v_2}{v_1'} d(\frac{v_2}{v_1'})}{1 - 2 \frac{v_2}{v_1'} + (\frac{v_2}{v_1'})^2 + 2(\frac{b}{\Delta L})s + (\frac{b}{\Delta L})^2 s^2 - 2 \frac{b}{\Delta L} s \frac{v_2}{v_1'}} \quad (29)$$

setting

$$s = x$$

$$v_2/v_1' = y$$

the following final differential equation can be formed

$$\frac{dy}{dx} = \frac{1}{k} \left[ \frac{1}{2y} - 1 + \frac{y}{2} + \frac{x}{y} \left( \frac{b}{\Delta L} \right) + \frac{x^2}{2y} \left( \frac{b}{\Delta L} \right)^2 - x \left( \frac{b}{\Delta L} \right) \right] \quad (30)$$

This equation can be solved by readily available computer methods (For the present evaluations the Runge-Kutta method on the Hewlett-Packard Calculator 9820a was used). Figure 4 compares the simplified method given by Equation 22 with the more accurate one expressed in Equation 30 for the same segment length in each case. One sees that the simplified method gives practically the same results as the more refined calculations. The agreement begins to suffer with the particle speed approaching the gas speed as can be seen from the upper curve with the smaller particle to gas density ratio, where the particle speed reaches about 75% of the gas speed. Since for the present calculations (Section V) the velocity ratios stay, in general, below this value, the simplified method was exclusively used in these calculations.

## 2. SEGMENT SELECTION

A simple relation is derived which allows a convenient selection of the segment length for the stepwise calculation of the expansion

process in a nozzle with a circular cross section. From the schematic drawing of a portion of an axisymmetric supersonic expansion nozzle shown in Figure 5 one can derive the following relations

$$\left(\frac{D_1}{D_2}\right)^2 = \frac{A_1}{A_2} \quad (31)$$

$$D_1 = D_2 - 2 L \tan \beta \quad (32)$$

These two relations can be combined to yield

$$\frac{A_1}{A_2} = \left(1 - 2 \frac{L}{D_2} \tan \beta\right)^2 \quad (33)$$

In this way the segment cross section ratio, as it enters the nozzle flow equations, is related to readily given nozzle geometry. For the subsonic portion of an expansion nozzle the corresponding equation is

$$\frac{A_1}{A_2} = \left(1 + 2 \frac{L}{D_2} \tan \beta\right)^2 \quad (34)$$

#### SECTION IV

#### NOZZLE HEAT LOSSES

The stepwise calculation of the gas expansion process provides ready conditions for the inclusion of heat losses through the nozzle wall. For the heat loss from a small nozzle segment one can write

$$\Delta Q_{\text{Loss}} = h \cdot D \cdot \pi \cdot \Delta L \cdot \Delta t \cdot \Delta T \quad (35)$$

This equation will be treated in more details. The heat transfer coefficient  $h$  in this relation is conveniently obtained with the help of the Reynolds analogy, which states (Reference 3)

$$\text{Nu} = \text{Re} \frac{(c_f)_{\text{wall}}}{2} \quad (36)$$

Then the heat transfer coefficient follows using the well known relation

$$(c_f)_{\text{wall}} = \frac{(c_f)_{\text{pipe}}}{4} \quad (37)$$

$$h = \frac{k \cdot v \cdot \rho_g}{\mu} \frac{(c_f)_{\text{pipe}}}{8} \quad (38)$$

Thus, we can introduce our previously used pipe friction coefficient. The time element  $\Delta t$  in Equation 35 stands for the residence time of the gas in the segment and is given by

$$\Delta t = \frac{\Delta L}{v} \quad (39)$$

The temperature difference  $\Delta T$  in Equation 35 is given by the relation

$$\Delta T = (T_1)_0 \delta_{\text{rec}} - T_{\text{wall}} \quad (40)$$

where  $\delta_{\text{rec}}$  is the wall temperature recovery factor. The remaining factors

in Equation 35 are the segment Diameter  $D$  and the segment length  $\Delta L$ . Therefore, Equation 35 using Equations 38 to 40 becomes

$$\Delta Q_{\text{loss}} = \frac{k \rho_g}{\mu} \frac{c_f}{8} D \pi (\Delta L)^2 [ (T_1)_o \delta_{\text{rec}} - T_{\text{wall}} ] \quad (41)$$

Due to the heat loss given by this equation the total gas temperature drops within the nozzle length  $\Delta L$

$$(T_2)_o = (T_1)_o - \frac{\Delta Q_{\text{loss}}}{c_p \cdot m} \quad (42)$$

In this equation  $m$  is the gas mass passing through the segment within the time element  $\Delta t$ . For the segment exit temperature one can write more explicitly

$$(T_2)_o = (T_1)_o - \frac{k c_f}{\mu c_p} \frac{\Delta L}{D} [ (T_1)_o \delta_{\text{rec}} - T_{\text{wall}} ] \quad (43)$$

The nozzle wall temperature in this equation must still be determined. Assuming water-cooled walls, i. e., a constant temperature on the outer nozzle wall, one can write based on the common heat conduction relation

$$T_{\text{wall}} = Q_{\text{Flux}} \frac{d}{k_{\text{Cu}}} + T_{\text{water}} \quad (44)$$

The heat flux occurring in this equation is readily obtained from the previously derived relation for the heat loss from the segment by writing

$$Q_{\text{flux}} = \frac{\Delta Q_{\text{Loss}}}{S \cdot \Delta t} \quad (45)$$

Since  $\Delta Q_{\text{Loss}}$  is a function of the wall temperature,  $Q_{\text{Flux}}$  is also a function of the wall temperature. To overcome this functional difficulty the nozzle calculations are started with an estimated wall temperature for the first segment of the nozzle.

Applying Equation 43 to consecutive segments of the nozzle the drop in total temperature over the whole nozzle length can be determined. The correction of the gas density as it is needed for calculating the particle acceleration can now be found from the total temperature with the pressure in the flow and the flow Mach number known from the previously derived flow calculations (Equations 16 and 19).

## SECTION V

### CALCULATION RESULTS

Figures 6 through 8 show the flow conditions, the particle velocities, and the heat losses calculated for a number of axisymmetric nozzle configurations for one set of operating conditions, which is only varied for Figure 8 where the particle injection point is moved downstream of the nozzle throat. The geometry given by Figure 6 for the subsonic and by Figure 7a for the supersonic nozzle portion is that of an experimental acceleration nozzle. All configurations have the same subsonic nozzle geometry as given in Figure 6, which provides the calculation results for the subsonic conditions. Figures 7a to c give the results for the supersonic nozzle portion for various nozzle geometries. The geometries are identified in the figures by a plot of the nozzle diameter over the nozzle length, which serves as abscissa in all presentations of the calculation results. The nozzle wall angle is also listed in the figures.

Nozzle wall friction and particle drag coefficients used for the present calculations are estimates based on generally available information on the subject. Typical Reynolds numbers for the present type of flow conditions are listed in Table 1.

TABLE 1  
REYNOLDS NUMBERS FOR FLOW CONDITIONS

Nozzle Pos. L	$Re_p$	$Re_f$
14 mm	940	104000
20	1300	117000
28	870	77000
41	700	68000
65	530	59000
116	350	49000

TABLE 1 (Continued)

## REYNOLDS NUMBERS FOR FLOW CONDITIONS

Nozzle Pos. L	$Re_p$	$Re_f$
241	180	37000
399	100	29000
602	60	22000
806	27	14000

For the subsonic portion of the expansion nozzles a friction coefficient of 0.02 (pipe friction coefficient) was chosen. For the supersonic portion the corresponding value is 0.015. Nozzle flow calculations presented in Reference 4 provided some special guidelines for these choices. An analysis on wall friction losses given in Reference 2 also influenced the choices. Though experiments with expansion nozzles having pertinent geometries were carried out, no direct comparison of actual gas or particle speeds with calculated values were possible due to the difficulties in reliably measuring velocities under the applicable extreme test conditions. However, in the present analysis the Reynolds analogy between friction and heat losses was used to determine nozzle heat losses and subsequently gas exit temperatures. Thus, a comparison of calculated and experimental gas temperatures provides a clue for the validity of the calculations. Circumstances did not allow exact gas temperature measurements in the present tests. However, from the glow color of an uncooled, 190 mm long, stainless steel, guide tube attached to the nozzle exit an estimate of the gas temperature was possible. The yellow-white glow color of the exit portion of the guide tube suggested a tube color temperature of 1400° to 1500°K. The calculated gas temperature at the nozzle exit ( $L = 660$  mm in Figure 7a) is 1600°K. Since the heat losses from the tube ( $\approx 0.06$  KW/cm<sup>2</sup>) were small compared to the heat flux from the gas ( $\approx 0.7$  KW/cm<sup>2</sup>), the tube end which is fairly far removed from the

tube attachment point, can be assumed to have nearly reached gas recovery temperature. Therefore, calculation and experiment agree within the order of 100°K, a value which allows one to conclude that the nozzle wall friction assumptions are reasonable.

For the part of the expansion nozzle where most of the particle acceleration occurs, the particle Reynolds number ranges from about 1300 near the throat down to about 100 at  $L = 400$  mm. The drag coefficient for a sphere in this regime ranges from about 0.4 to 1.0. Since the actually used particles (graphite pellets) deviated from a spherical shape and had no smooth surface, a drag coefficient near the upper limit was chosen with a value of 0.8. For simplicity this value was also applied to the nozzle exit region where the particle approaches the Stokes flow regime.

Figures 7a to c show that the obtainable particle velocity is not greatly affected by the nozzle geometries considered in these figures. The particle to gas velocity ratio never exceeds a value of around 0.5 except in the regions where the gas velocity drops from its peak value. In all cases the particle velocity increases very slowly in most of the downstream portion of the supersonic expansion region.

For selecting the best nozzle geometry the obtainable particle velocities must be compared for the expansion pressure ratio given by the experimental conditions. In the present case this ratio is determined by the permissible arc heater operating pressure ( $100 \text{ kg/cm}^2$ ) and ambient conditions ( $1 \text{ kg/cm}^2$ ) preferred for carrying out the erosion experiments. Resulting particle velocities are listed in Table 2. This table gives an overview for the general possibilities of accelerating 80-micron particles in an expanding gas. Cases No. 1 to 3 pertain to the conditions given in Figures 7a to c. For the largest pressure ratio possible with the present experiments ( $p/p_0 = 0.01$ ), the maximum particle velocity is obtained in Case No. 2 with a  $0.5^\circ$  wall angle for the supersonic nozzle portion. This velocity of 2002 m/sec is only slightly better than the ones obtained in Cases No. 1 and 3. The particle velocities given for

pressure ratio 0.02 are indicative for the conditions where the nozzles are cut off before ambient pressure is reached. The particle velocities are only slightly reduced in these cases.

The remaining cases in Table 2 serve to demonstrate the practicality of choosing the small size nozzles given by Cases No. 1 to 3 and dealt with in details in Figures 7a to c. Cases No. 4 to 7 show that higher particle velocities can be obtained by increasing the nozzle size and consequently the nozzle mass flow. For the same particle residence time in the gas the relative wall friction influence is reduced. By doubling the nozzle cross-sectional areas (Cases No. 4 and 5) some gain in particle velocity is obtained. In view of the associated increase in cost of already expensive equipment and operating medium the worthwhileness of the improvement is questionable. A further doubling of the nozzle cross-sectional areas (Cases No. 6 and 7) produces a further increase in particle velocity. However, cost may become prohibitive in these cases.

Cases No. 8 and 9 show examples with air as the operating medium. Due to its higher molecular weight air cannot be expanded to as high a velocity as helium, however, its higher density provides a better drag coupling between particle and gas (Equation 22). Thus, air is of some interest for accelerating 80-micron particles. Case No. 8 is the same as Case No. 3 with air replacing helium as operating medium. Only the air velocities are listed for air. Survey calculations indicated that due to the superior coupling in this case the particle velocities approach closely the air velocities. This closeness makes the present method of calculating particle velocities invalid. The air velocities listed in Table 2 serve as upper limit for the particle velocities. Even the air velocities stay substantially below the particle velocities obtained with helium.

Case No. 9 deals with the practical possibility of using a large scale air expansion nozzle with increased plenum pressure ( $200 \text{ kg/cm}^2$ ). To stay near practical limits the plenum temperature is reduced to  $2000^\circ\text{K}$ . Compared to Case No. 8 the air velocities are substantially increased but

still appreciably below the particle velocities obtained with the much smaller helium operated nozzles.

The drop in gas velocity in the downstream portion of the supersonic nozzle is caused by the large drop in the gas stagnation temperature due to the heat loss from the nozzle. The figures show that the expansion Mach number still increases throughout the nozzle though mostly at a very small rate caused by the accumulative effect of wall friction. An increasing Mach number is a requirement for maintaining supersonic flow stability in the nozzle.

In the throat region the heat flux to the nozzle wall reaches a maximum of about  $10 \text{ KW/cm}^2$ . This enormous heat flux calls for particular attention in the design of the nozzle cooling system. The step down in the heat flux seen in the curves at the nozzle throat is simply caused by the change of the wall friction coefficient from 0.02 for the subsonic nozzle portion to 0.015 for the supersonic portion.

Figure 8 shows the case given in Figure 7a with the point of particle injection moved downstream of the throat. In spite of the delayed injection the final particle speed is reduced only slightly from the case shown in Figure 7a. As a general observation one can say that in all cases treated here, the particles are very rapidly accelerated to about half the gas velocity but further acceleration then becomes increasingly sluggish.

## SECTION VI

### FLOW PROFILE CONSIDERATIONS

#### 1. GENERAL DISCUSSION

The present flow calculation method is set up to find for a given duct the flow momentum at the exit of the duct from the flow conditions at the inlet. The result is expressed in the form of an effective Mach number. This Mach number represents average flow conditions which in accordance with its derivation fulfills the condition of continuity in the flow through the duct. Since the definition of the pipe friction coefficient is based on the use of such average flow conditions as a reference, the effective Mach number is the right choice for determining the friction forces (Reference 3).

For the particle acceleration it is of interest to obtain information about the particle velocity distribution over the flow cross section, in particular, about the peak velocities of the particles. In a first approximation the particle velocity distribution at the nozzle exit can be considered as directly proportional to flow velocity distribution, i.e., it is sufficient to determine the particle velocity distribution from the flow velocity distribution by simply using the particle to gas velocity ratio found in the calculations for the nozzle exit as a proportionality factor for the two distributions. For finding the peak particle velocity by this process a method is presented in the following which allows one to derive the peak Mach number from the effective Mach number for a given flow profile shape.

#### 2. PEAK MACH NUMBER

If the flow profile shape is given, the peak Mach number can be uniquely related to the effective Mach number by the requirement that for each Mach number distribution the flow momentum must be the same

as expressed by the relation

$$\int_0^A \gamma p M_p^2 dA = \gamma p M_{eff}^2 A \quad (46)$$

where  $\gamma$  and  $p$  are considered constants. The flow profile shape is considered to be given in the form of a Mach number distribution over the radius of a circular cross section. Determining the peak Mach number is a simple geometric problem. For the present purpose the shape of the profile is presented in terms of the square of the Mach number and assumed to be the frustrum of a cone. Then the specific problem is, as illustrated in Figure 9, to find the height of the frustrum which has the same volume as a cylinder the height ( $h_s + h_2$ ) of which is given. Practical relations are derived in the following.

The  $M^2$  - profile is given by the two ratios

$$\frac{d_0}{d_2} \quad \text{and} \quad \frac{h_s}{h_t}$$

The basic condition for deriving the relations is

$$\frac{h_s + h_2}{h_t} = \left( \frac{M_{eff}}{M_{max}} \right)^2 \quad (47)$$

For establishing a relation between  $h_s$  and  $h_t$  an auxiliary parameter is selected

$$a = \frac{d_0}{d_1} \quad (48)$$

The following geometric conditions must be fulfilled

1. from Equation 46 Volume  $V_1$  = Volume  $V_2$
2. from similarity  $\frac{h_0}{d_0} = \frac{h_0 + h_1}{d_1} = \frac{h_0 + h_1 + h_2}{d_2} \quad (49)$

From these conditions one can derive

$$\left(\frac{d_2}{d_1}\right)^3 = 3 \left(\frac{d_2}{d_1}\right) - (1 + a^3) \quad (50)$$

The solution to this relation is

$$\frac{d_2}{d_1} = 2 \cos\left[\frac{1}{3} \arccos\left(-\frac{1 + a^3}{2}\right)\right] \quad (51)$$

With Equation 51 the auxiliary parameter  $a$  is now directly connected to the above given  $M^2$  - profile description considering that

$$a \frac{d_1}{d_2} = \frac{d_0}{d_2} \quad (52)$$

Simple geometric similarity now allows all magnitudes of the profile scheme in Figure 9 to relate to each other. In particular, Equation 47 can now be conveniently written

$$\left(\frac{M_{\text{eff}}}{M_{\text{max}}}\right)^2 = \frac{\frac{h_s}{h_2} + 1}{\frac{h_1}{h_2} + 1 + \frac{h_s}{h_2}} \quad (53)$$

where the occurring ratio values on the right side are related to the given profile conditions by

$$\frac{h_1}{h_2} = \frac{1 - a}{\frac{d_2}{d_1} - 1} \quad (54)$$

$$\frac{h_s}{h_2} = \frac{\frac{h_s}{h_t} \frac{h_1}{h_2} + 1}{1 - \frac{h_s}{h_t}} - 1 \quad (55)$$

Equations 51 through 55 allow one to prepare a plot as shown in Figure 10. The flow profiles shown in this figure give the direct Mach number profiles over the duct diameter instead of the square values as originally expressed in Figure 9. Figure 10 covers all geometric conditions with which flow profiles can be expressed. Actually occurring flow profiles can be identified with those occurring along very low values of  $M_{wall}/M_{max}$  except for high  $d_1/d_2$  values, where large Mach number ratios are possible characterizing the flow profile start-up at the inlet to a duct. Note: in Figure 10 notation  $d_0$  is changed to  $d_1$ .

## SECTION VII

## CONCLUSIONS

The acceleration of  $80\mu$  diameter particles in expanding helium to near 60% gas velocity for the purpose of re-entry erosion testing requires the use of expansion nozzles which have a length in the order of 100 nozzle throat diameters. Wall friction incurred in such nozzles becomes a limiting factor for the effectiveness of this acceleration process. To account for the friction influence in the design of these nozzles the expansion process is conveniently expressed in terms of the occurring fluid forces. This procedure allows a ready inclusion of the friction forces which by themselves can be determined with the help of known wall friction coefficients. This calculation method yields a particularly accurate account of the friction effects if applied consecutively along the nozzle to small nozzle segments. This stepwise calculation procedure also accommodates the determination of the heat losses from the nozzle and provides a basis for calculating the particle acceleration process. The segment length can be adjusted to the rapidity of the flow changes as it is particularly necessary in the nozzle throat region due to the extreme sensitivity of the flow to cross section changes in this region. Very small segments must be chosen to stay within the validity of the assumptions made for the calculations.

The present flow calculation process does not include detail boundary layer considerations. Instead it accounts for viscous effects in terms of a wall friction coefficient. In spite of this simplification a consistent description of the flow process is possible as long as the chosen friction coefficient is sufficiently representative for the viscous conditions in the flow or if the coefficient is only used as a parameter to demonstrate its influence on the flow. For the present purpose of comparing particle velocities obtained with only slightly changed nozzle geometries the exact representation of the viscous conditions was not considered essential and constant friction coefficient values only different for subsonic and supersonic flow were chosen.

The end results of the present flow calculations give the flow exit momentum expressed in terms of an average flow Mach number which may also be called effective Mach number. Assumptions about the flow profile are necessary to determine the peak flow Mach number. For the present determination of particle velocities this effective Mach number was used.

In calculating nozzle designs for accelerating small particles (0.08 mm) to high velocities (2000 m/sec) one finds that it is difficult to obtain particle velocities much larger than 50% of the occurring maximum gas velocities. Due to the wall friction influence in the long expansion nozzles (0.7° - 1.4° opening angle for the supersonic nozzle portion) less than 50% of the isentropic expansion velocity can be obtained for the average accelerating gas velocity. Since extreme high gas temperatures (arc heated gas) must be employed to obtain sufficiently high gas velocities (at an expansion pressure ratio of 100 and helium as operating medium) the expansion nozzles are exposed to extreme heat loads (10KW/cm<sup>2</sup> in the throat region) requiring intense water cooling of the nozzles. Enthalpy losses ranging from 30% to 50% of the initial enthalpy occur during expansion.

REFERENCES

1. S. Hasinger, Performance Characteristics of Ejector Devices, Aerospace Research Laboratories, Technical Report ARL-TR-75-0205, Wright-Patterson AFB, Ohio, June 1975.
2. S. Hasinger, Analysis and Design of a Supersonic Radial Outflow System, Flight Dynamics Laboratory, Air Force Wright Aeronautical Laboratories, Technical Report AFWAL-TR-80-3028, Wright-Patterson AFB, Ohio, October 1980.
3. H. Schlichting, Boundary Layer Theory, McGraw-Hill, New York, 6th Ed. p. 662.
4. High Speed Aerodynamics and Jet Propulsion, Volume III, "Fundamentals of Gas Dynamics", Princeton University Press, p. 157, 1958.

TABLE II

## CALCULATION RESULTS

No.	Throat Diam. mm	Nozzle Wall Angle subs.	supers.	$p/p_o = 0.02$			$p/p_o = 0.01$			$p/p_o = 0.005$		
				L mm	$v_g$ m/sec	$v_p$ m/sec	L mm	$v_g$ m/sec	$v_p$ m/sec	L mm	$v_g$ m/sec	$v_p$ m/sec
Helium ( $\gamma = 1.666$ )												
				$T_o = 3200^\circ K$								
				$p_o = 100 \text{ atm}$								
1.	4.02	7°	0.34°	1032	-	1959	1590	-	1962	see Figs. 7a to c		
2.	4.02	7°	0.5°	602	-	1976	940	-	2002			
3.	4.02	7°	0.7°	404	-	1935	607	-	1978			
4.	5.91	10°	0.5°	860	-	2193	1349	-	2216	no 0.34° section		
5.	5.91	10°	0.7°	530	-	2140	825	-	2192			
6.	8.4	7°	0.7°	766	-	2350	1203	-	2383			
7.	8.4	15°	1.0°	450	-	2235	680	-	2309			
Air (heated, $\gamma = 1.32$ )*												
				$T_o = 3200^\circ K$								
				$p_o = 100 \text{ atm}$								
8.	3.94	7°	0.7°	380	1486	-	584	1430	-	882	1566	-
Air (heated, $\gamma = 1.32$ )*												
				$T_o = 2000^\circ K$								
				$p_o = 200 \text{ atm}$								
9.	20.1	20°	5°**	220	1638	-	307	1700	-	423	1745	-

\*) In the calculations for air only rough approximations for the thermodynamic properties of heated air were used.

\*\*) Minimum angle for maintaining supersonic expansion at  $c_f = 0.015$ .

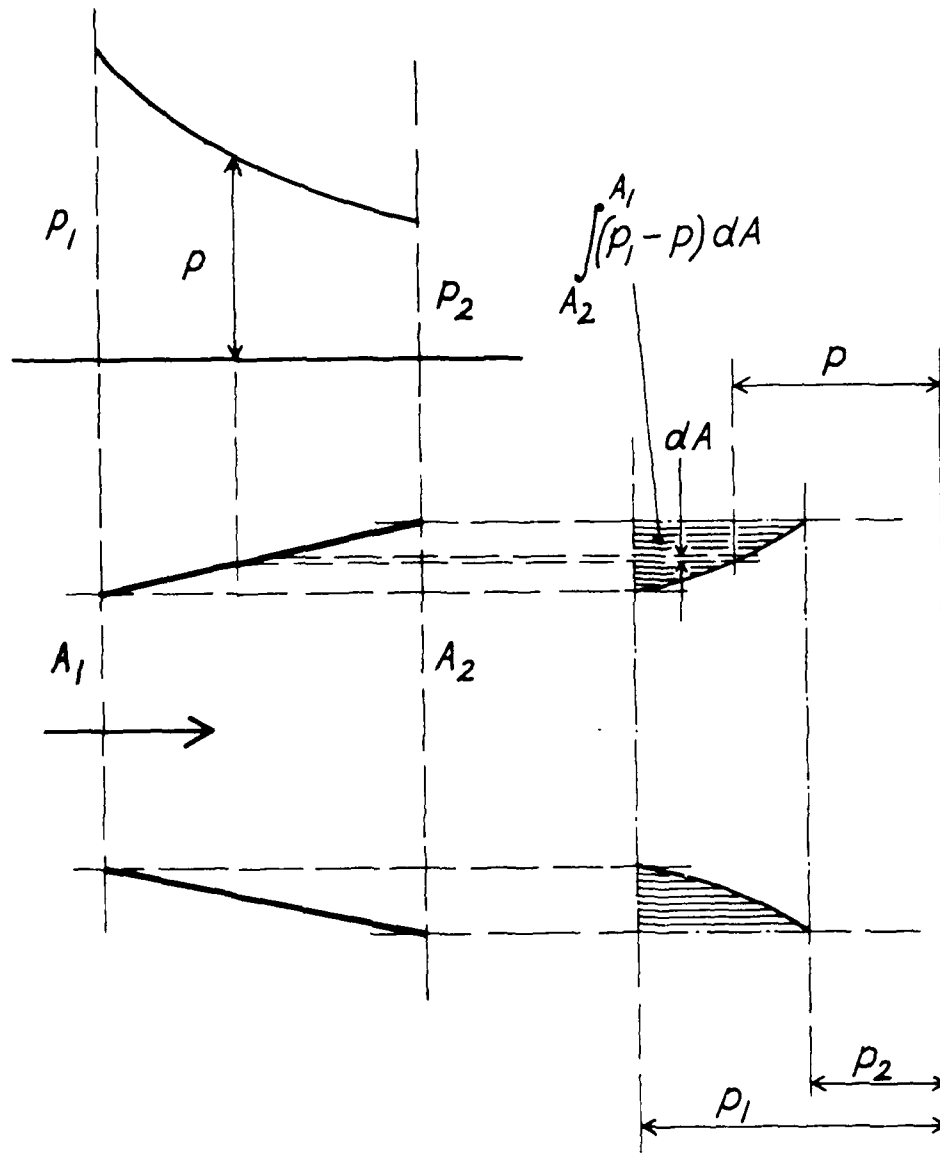


Figure 1. Fluid Pressure Forces in a Flow Duct Element (Supersonic Expansion)

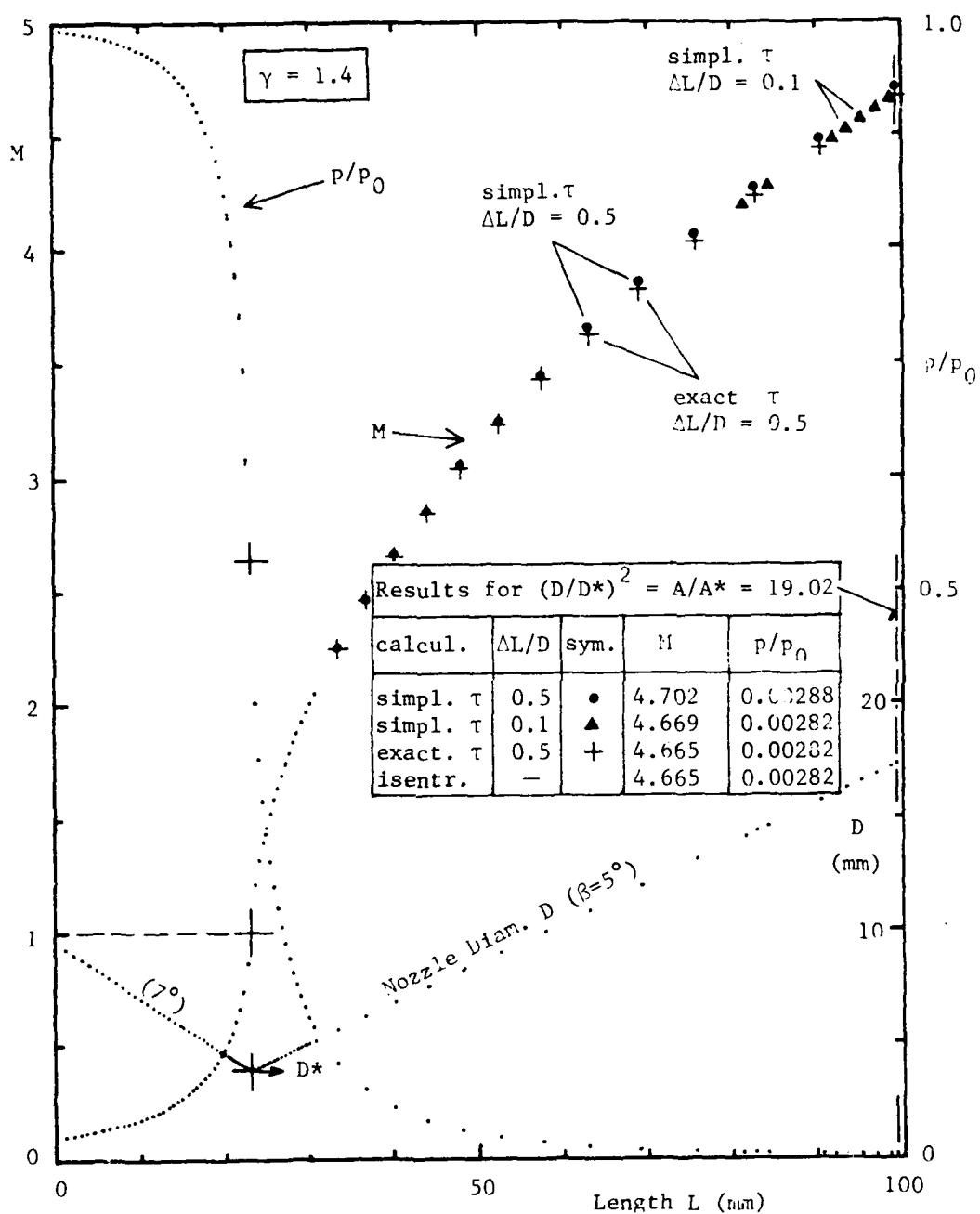


Figure 2. Comparison of Segmental Flow Calculations with Isentropic Flow Conditions for Zero Wall Friction ( $\gamma = 1.4$ ). (For clarity, curve points for the smaller segment length have been largely omitted in the supersonic region. Differentiating markings of curve points have been applied only in the supersonic region and only for the Mach number curve where results deviate sufficiently).

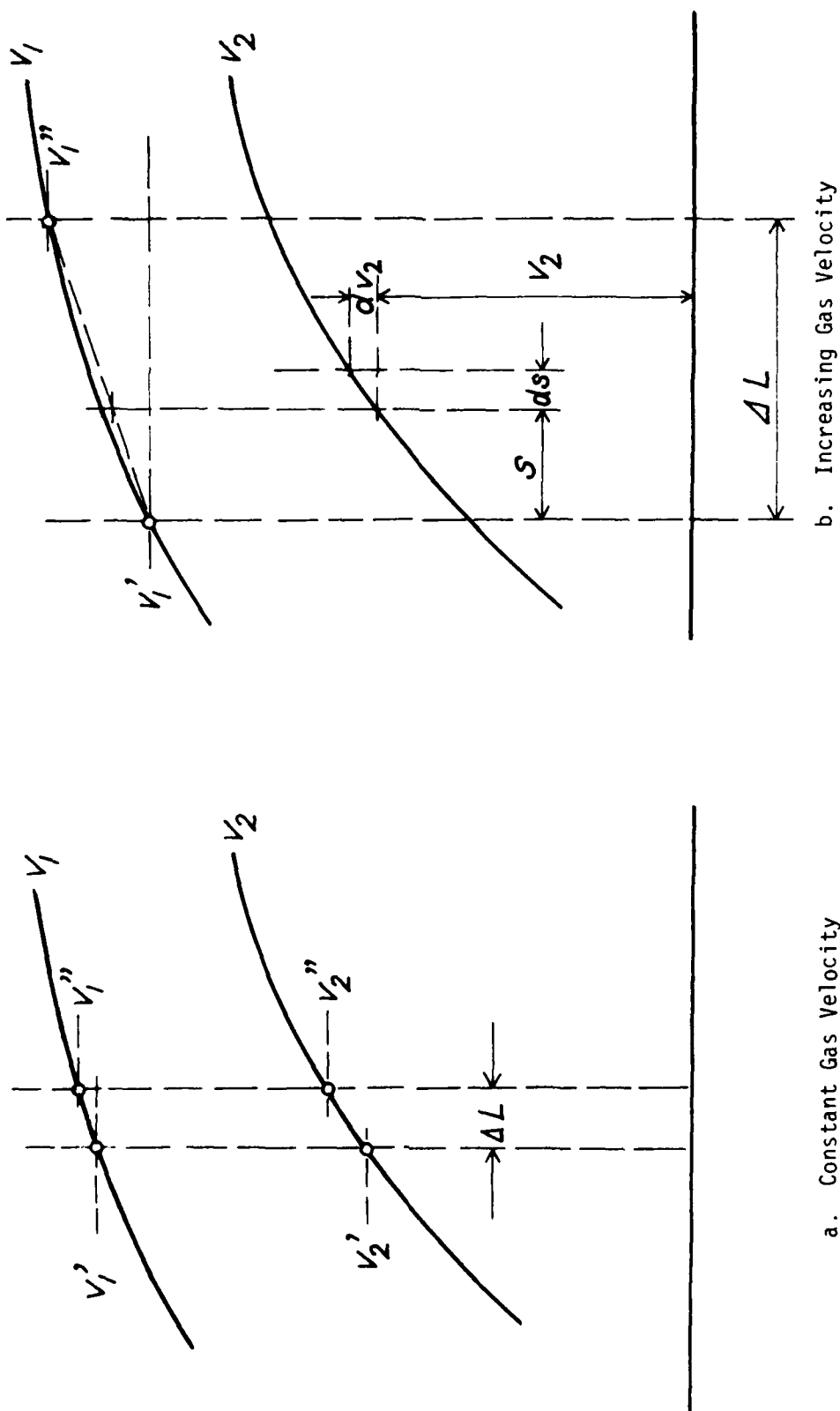


Figure 3. Particle Acceleration Models

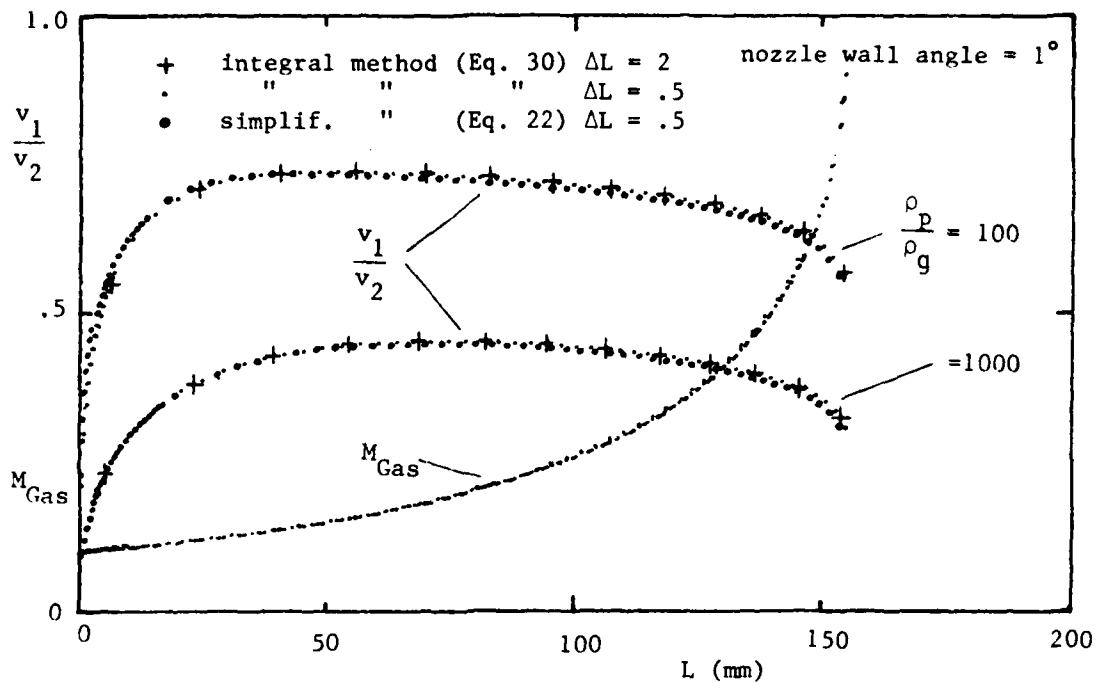


Figure 4. Particle Accelerations Calculated with the Simplified Method (Illustrated in Figure 3a and Used for the Example Calculations in Section V) Compared with Results Obtained with the More Accurate Method Illustrated in Figure 3b.

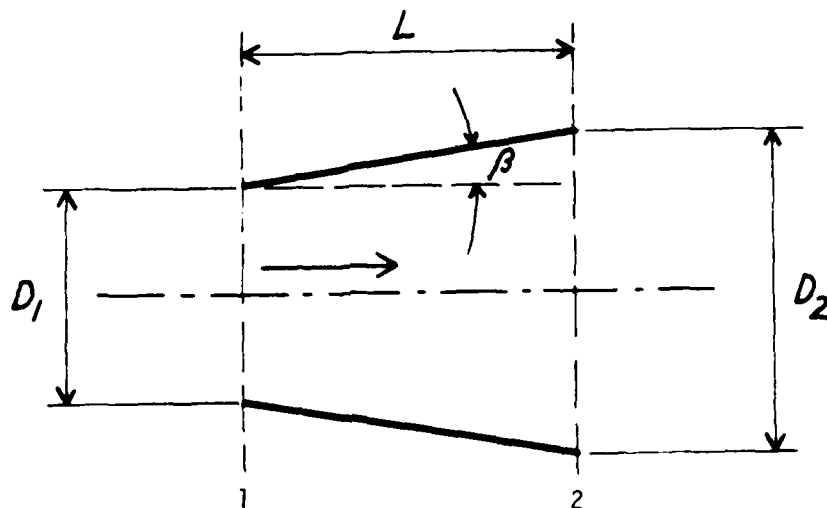


Figure 5. Segmental Axisymmetric Nozzle Geometry

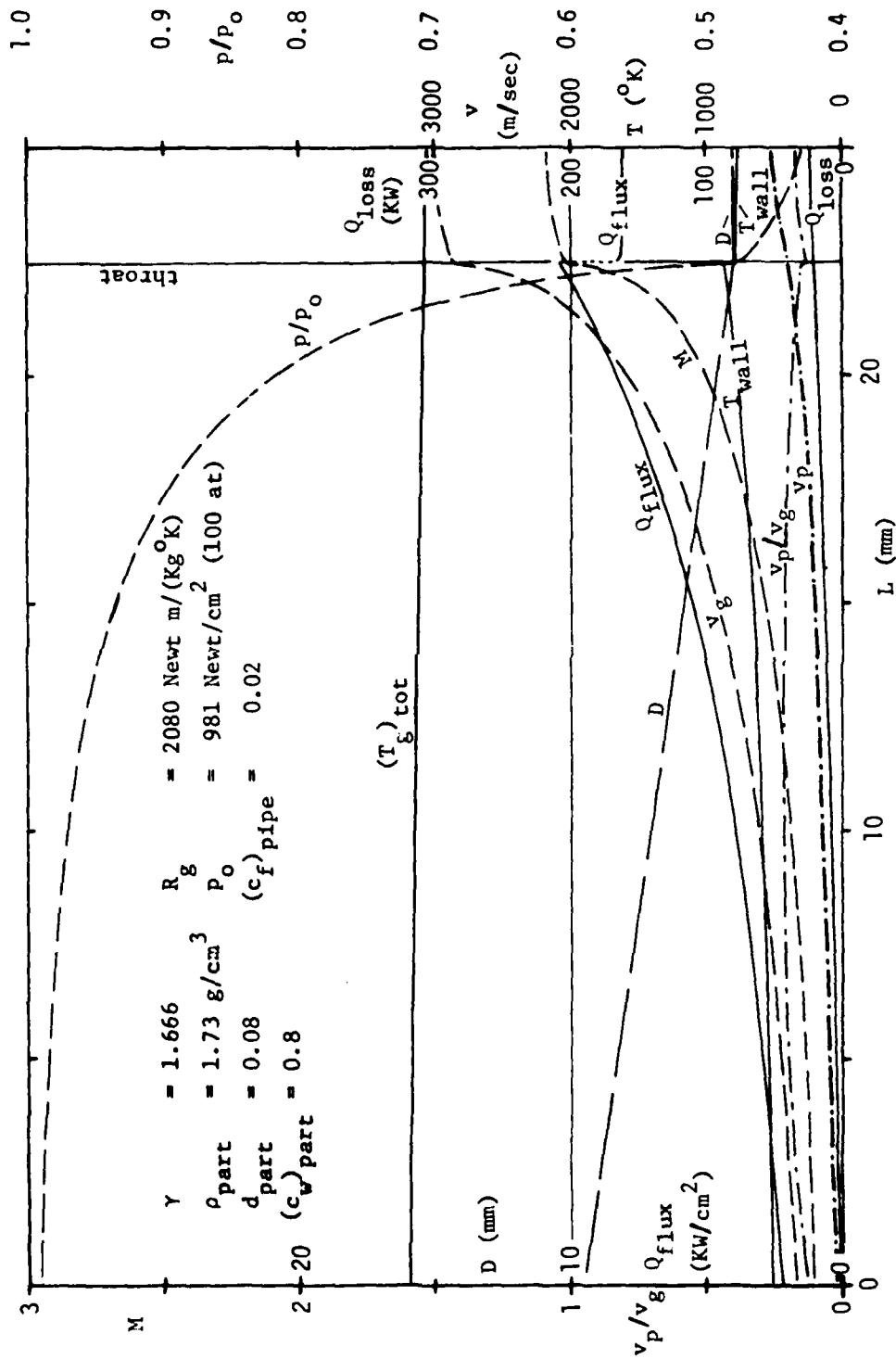


Figure 6. Flow Conditions, Heat Loss, and Particle Acceleration for the Subsonic Portion of the Expansion Nozzles Considered in Figures 7a to c for Their Supersonic Nozzle Portions

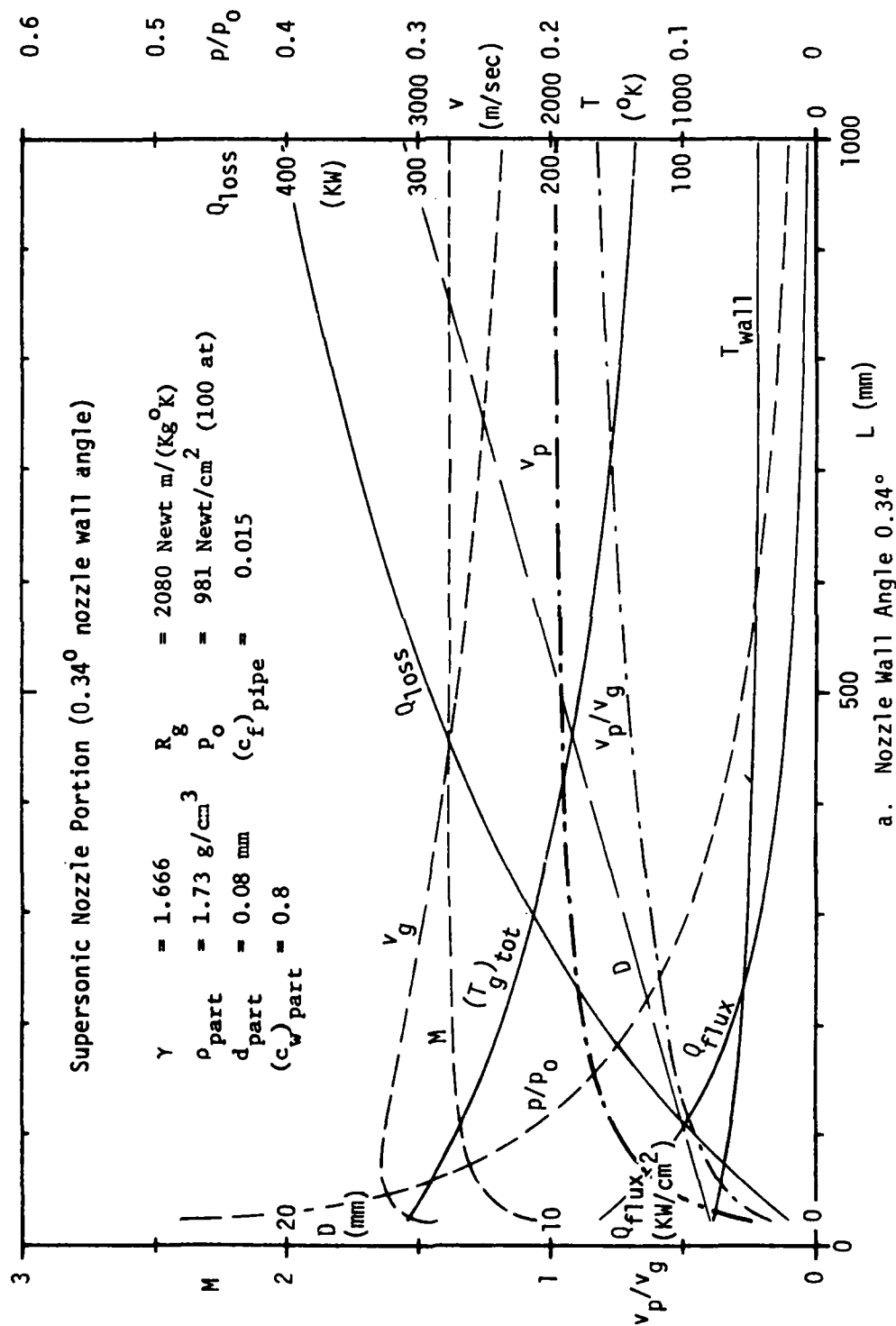
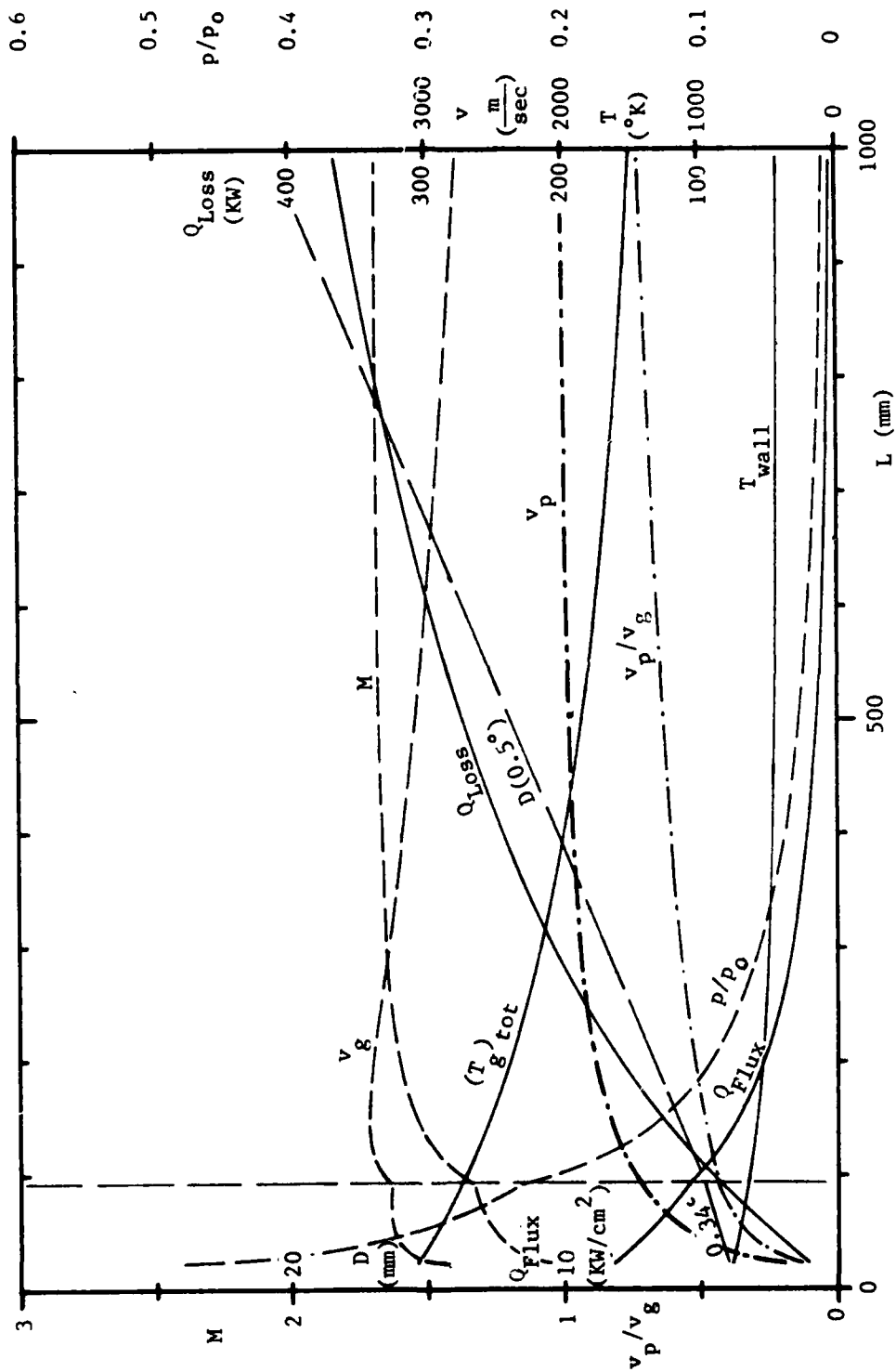
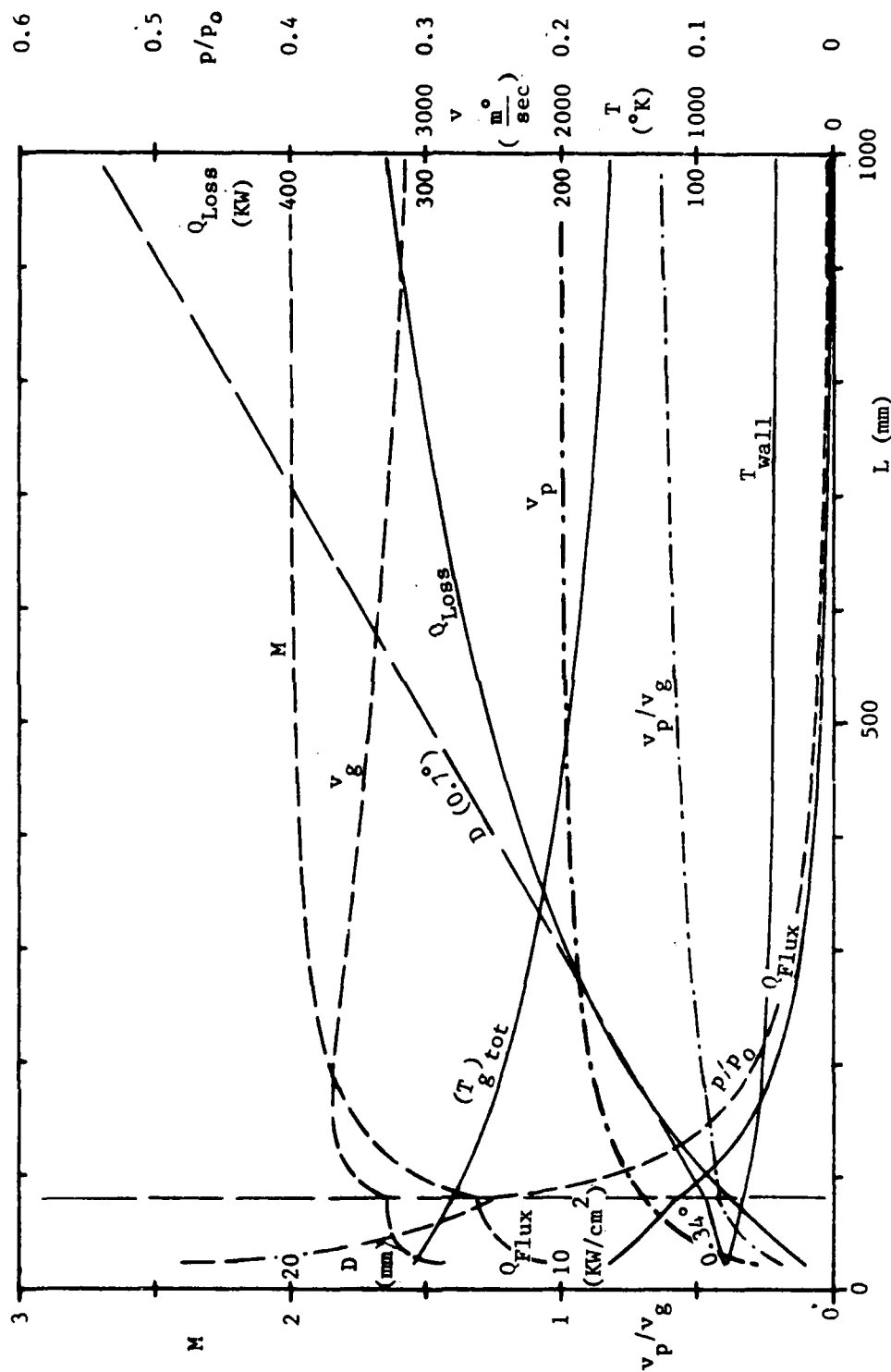


Figure 7. Flow Conditions, Heat Loss, and Particle Acceleration for Various Supersonic Nozzle Configurations (For Subsonic Nozzle Portion See Figure 6)



b. Nozzle Wall Angle  $0.34^\circ$  and  $0.5^\circ$



c. Nozzle Wall Angle  $0.34^{\circ}$  and  $0.7^{\circ}$

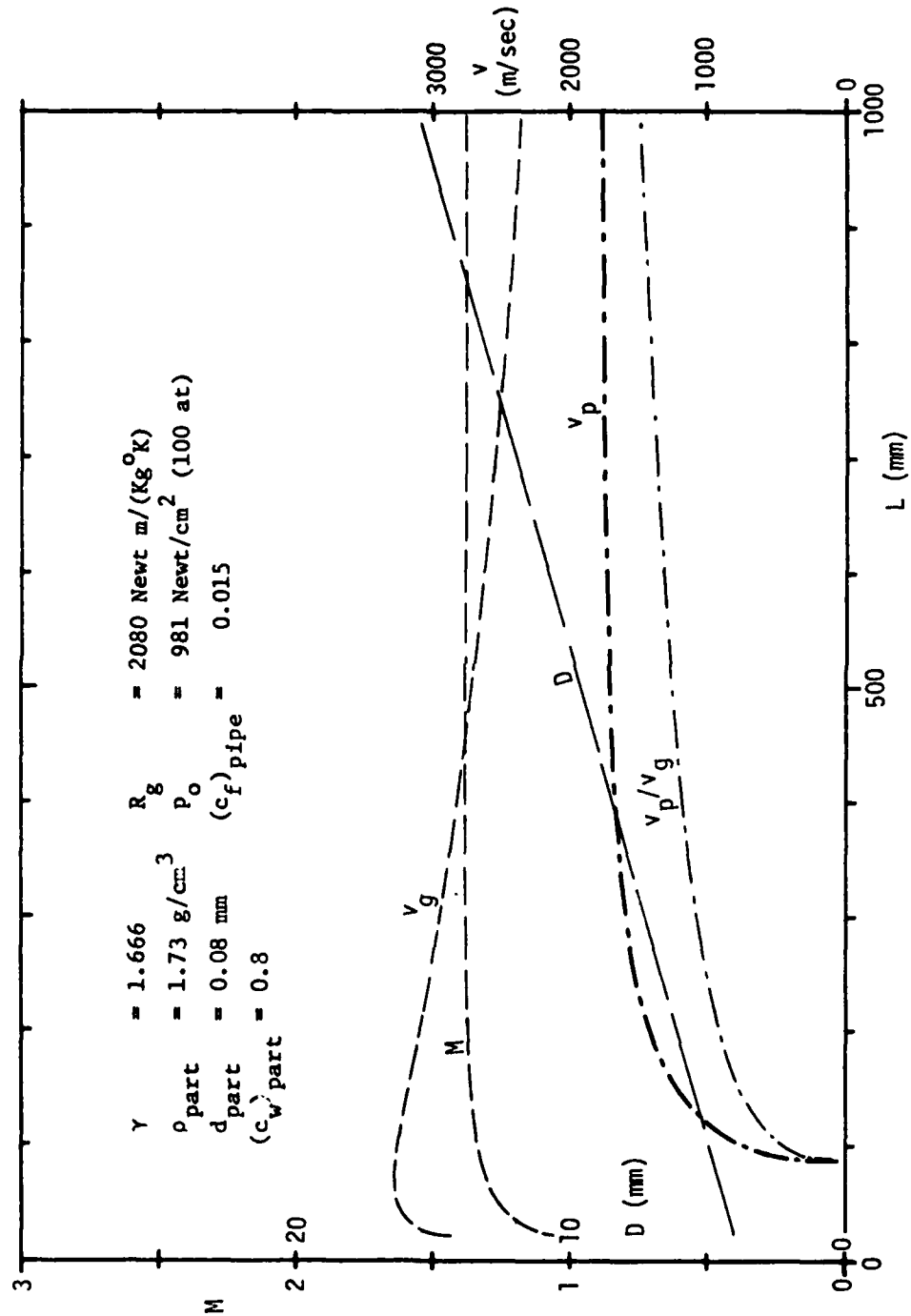


Figure 8. Case of Figure 7a with Particles Injected Downstream of the Nozzle Throat.

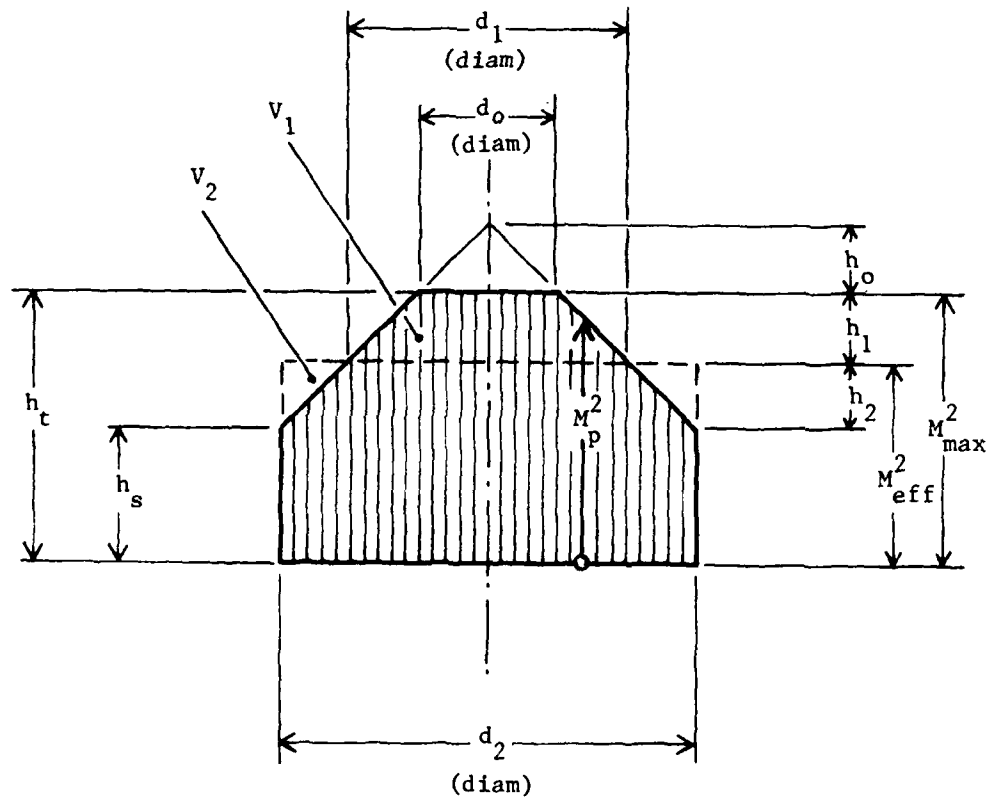


Figure 9. Schematic Flow Profile (in terms of  $M_p^2$ )

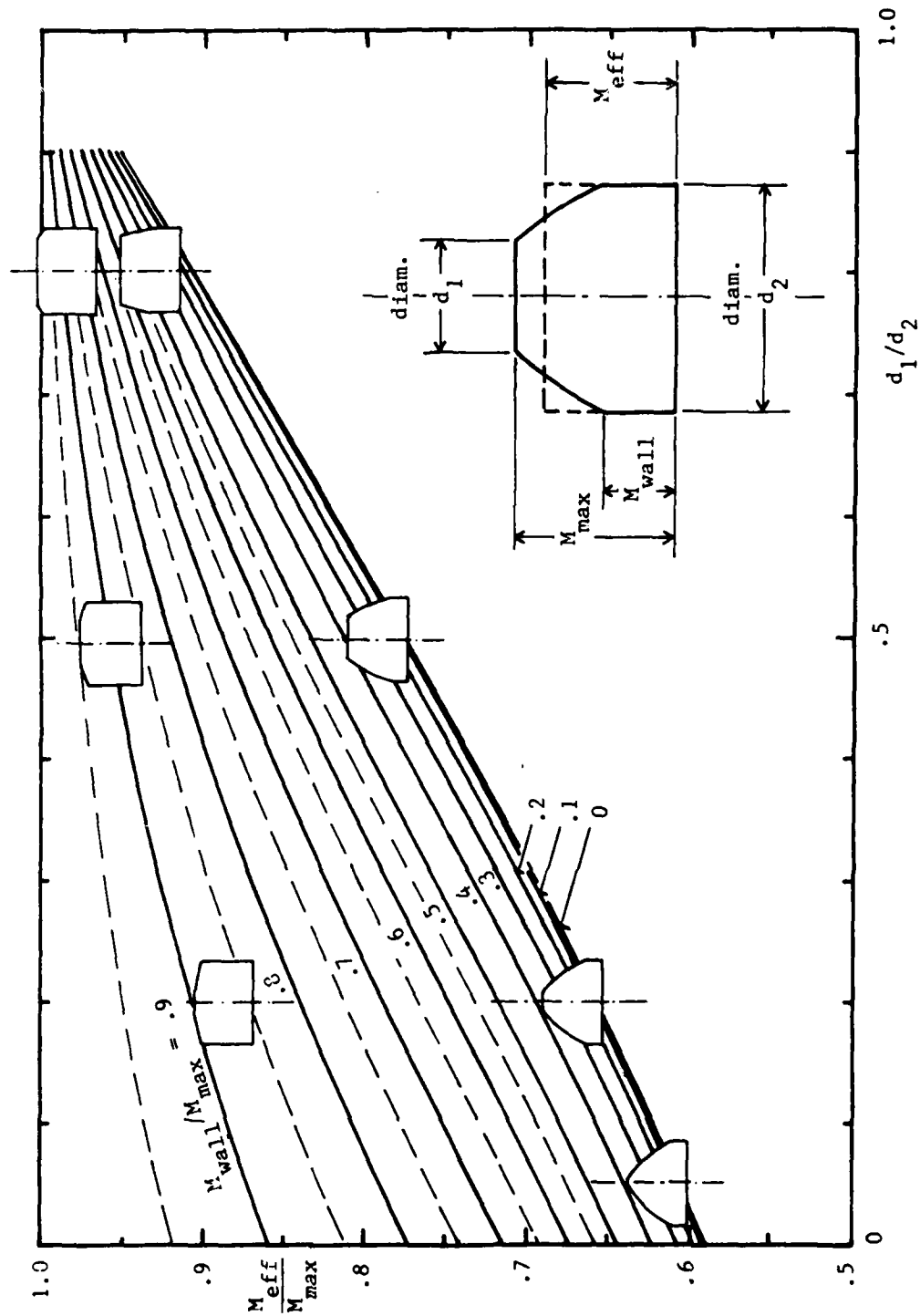


Figure 10. Plot for Determining Peak Mach Numbers from Effective Mach Numbers for Given Flow Profile Shapes